Int. J. Econ. Environ. Geol. Vol. 11 (1) 24-34, 2020
Journal home page: www.econ-environ-geol.org

Open Access
ISSN: 2223-957X

Occurrence of a Likely Tuff Bed between the Middle and Upper Siwaliks, Taunsa area, Dera Ghazi Khan, Eastern Sulaiman Range, Pakistan

Rahman Ullah,[1,2*] Nie Fengjuin[1], Zhang Xin[1], Zhang Chengyong[1], Saqib Izhar[2], Idrees Safdar[2], Asim Ali[1,2]

[1]State Key Laboratory of Nuclear Resources and Environment,
East China University of Technology, Nanchang, Jiangxi, China
[2]Atomic Energy Minerals Centre, Lahore, Pakistan

*****Email: rahmanullah_mdn@yahoo.com

Received: *28 January, 2020* ***Accepted:*** *18 May, 2020*

Abstract: A likely tuff bed lies along the gradational contact of the Middle and Upper Siwaliks in eastern Sulaiman Range, Taunsa area of Dera Ghazi Khan district, Pakistan. This tuffaceous unit is 0.5–3 m thick and extends for 10 km along the north-south strike in the eastern limb of the Zindapir anticline. It is greyish white to white on fresh surface, fine-grained to silty at the bottom and clayey at the top and thus shows a fining upward grain-size grading. The lower part of the ash bed shows a prominent lamination defined by megascopically visible abundant biotite, while the central and upper parts are so fine-grained that the individual minerals cannot be seen in hand sample. Unlike the lower well-laminated part, the central and upper parts are crudely laminated to apparently massive. The bulk samples analysed with X-ray diffraction consist of quartz, feldspar (plagioclase), biotite, clays, calcite and some ore mineral likely spinel, while the clay-size fractions contain illite, chlorite, biotite and probably their mixed-layered varieties. The colour, texture, presence of abundant biotite and stratigraphic position of the Taunsa tuff correlate with those reported from Potwar plateau and from Kashmir basin. However, the apparent absence of smectite from the XRD pattern makes the Taunsa ash bed different from both Potwar and Kashmir tuffs. The present stratigraphic position of the tuff bed corresponds to shallow diagenetic zone, while the absence of smectite in the tuff and crystallinity of illite suggest that the tuff is probably derived upon reworking from a deeper diagenetic zone belonging to a lower stratigraphic level. The Eocene or other older pre-Siwalik units in Pakistan may have or had some primary ashfall deposits as reported in the northwestern Himalayas of India. This older volcanic ash may have been reworked to its present site of occurrence along the gradational contact of the Middle and the Upper Siwaliks in Taunsa area of Dera Ghazi Khan. However, the primary source of the Taunsa tuff may belong more likely to Chagai arc in Pakistan than to Dacht-e-Nawar volcanic complex in Afghanistan.

Keywords: Tuff, mineralogy, illite, chlorite, biotite, Siwaliks, Sulaiman Range, Pakistan.

Introduction

Sulaiman range is a conspicuous tectonic feature on the northwestern margin of the Indo-Pakistan plate (Fig. 1). Transpressional tectonics along Chaman Transform fault, a product of oblique collision of the Indian plate with the Afghan block, led to the formation of Sulaiman and Kirthar ranges (Fig. 1) (Humayon et al., 1991; Jadoon et al., 1994). A variety of structural models have been proposed for the origin and evolution of Sulaiman Range such as passive roof duplex geometry of thrusts (Banks and Warburton, 1986), flower structure (Kemal et al., 1991), sandbox model (Haq and Davis, 1997), thick-skinned tectonic model (Iqbal and Helmcke, 2004), pop-up reverse faults model (Asim et al., 2014; Saif-Ur-Rehman and Zaib, 2020). Sulaiman Range is composed of Triassic to Pleistocene sediments of both marine and continental origin including Siwalik molasse deposits with a thickness of ~3000 m (Ahmad and Khan, 1991). Siwalik sediments in the Sulaiman Range are distinguished in stratigraphic order as Vihowa, Litra and Chaudhwan formations (Fig. 2), which are mainly mudstones, sandstone, and conglomerate facies, respectively.

Bentonites, believed to have formed by alteration of volcanic ash, were recognized in Siwalik Group in both southwestern Kashmir basin (Middlemiss, 1930; Bhola, 1948) and Salt Range (Johnson et al., 1982). These previously reported bentonites were investigated for fission track dating (Johnson et al., 1982). The possible extension of the bentonites into Jammu area was studied by a number of researchers (Bhat et al., 2008, references therein). All these bentonites are considered to have resulted from alteration of ashfall deposits sourced from Dacht-e-Nawar volcanic complex near Kabul, Afghanistan (Johnson et al., 1982). The volcanic rocks of Chagai arc in Balochistan (Fig. 1) range in age from Cretaceous to Quaternary (Khan et al., 2010; Nicholson et al., 2010). However, they were not considered to have supplied ash to the Quaternary bentonite occurrences in Kashmir basin and Potwar plateau because of the more aerial distance of Chagai arc than Dacht-e-Nawar complex (Johnson et al., 1982). The initial Cretaceous to Paleocene volcanism in Chagai arc is tholeiitic, and from the Eocene onwards, it becomes calc-alkaline in nature (Siddiqui et al., 2015).

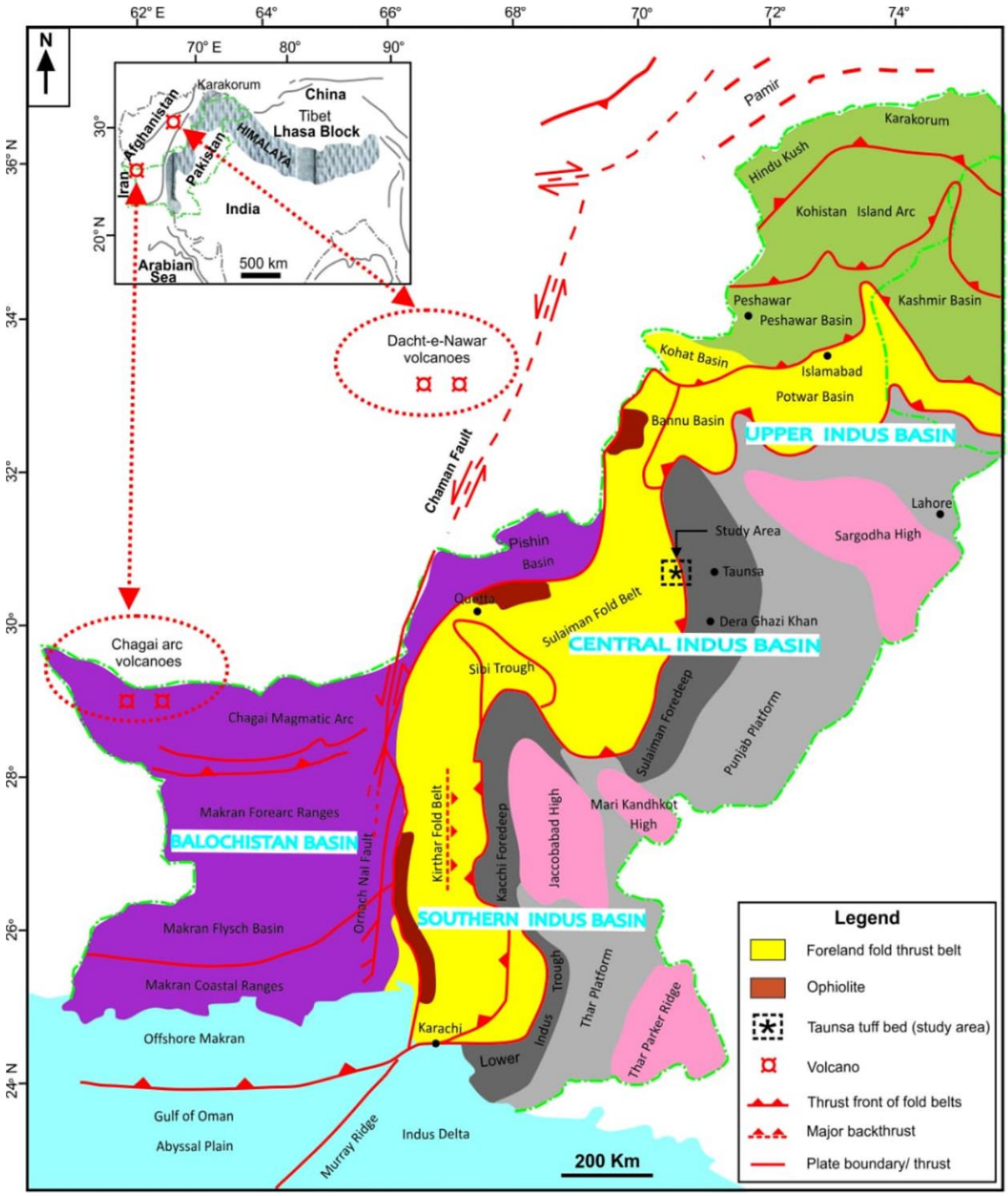

Fig. 1 Tectonic and sedimentary basin map of Pakistan (modified from Aziz and Khan, 2003). Inset shows Himalayan range and Dacht-e-Nawar volcanoes in Afghanistan (modified from Najman, 2006).

The late Cretaceous Bibai Volcanics in western Sulaiman range consist of basaltic rocks with abundant volcanic ash of tholeiitic composition (Kazmi, 1988; Siddiqui et al., 2010).

The volcanic ash bed of Taunsa area is exposed along the transitional contact of the Litra and Chaudhwan formations (Fig. 2) in the eastern limb of the Zindapir anticline in the eastern Sulaiman Range. This tuff bed was first reported in 2001 by the geologists of Pakistan Atomic Energy Commission, and was later identified as fuller's earth by Arif et al. (2005) investigating only two samples.

The current investigation is more systematic and detailed and takes into account field observations of the tuff and its petrographic, geochemical (unpublished), and mineralogical details through X-ray diffraction. However, this paper discusses only field observations, and the bulk and clay mineralogy of tuff bed with X-ray diffraction.

Materials and Methods

Field observations of the tuff bed were noted such as colour variations, texture and sedimentary structures, and its megascopically identifiable minerals. Nine samples were collected from the tuffaceous unit along a strike length of 10 km from its well-exposed, >1 m thick sections. In order to check for mineralogical variation, three samples with A, B and C nomenclature were collected from the lower, middle and upper parts of the bed, respectively. Where the tuff was poorly exposed, only one sample was collected preferentially from its central part to get its original mineralogy, i.e., one which is free of any intermixing of the tuff with the lower (sandstone) and upper (mudstone) facies.

The bulk samples were air dried, then crushed and ground to powder. In order to determine clay mineralogy, clay mineral fractions of three of the collected samples (ZV-80N-28A, -28B, and -28C) were obtained following the sedimentation method of Jackson (1978). These samples were treated with 20% acetic acid and 3% H_2O_2 to remove organic and carbonate matter, respectively following the standard

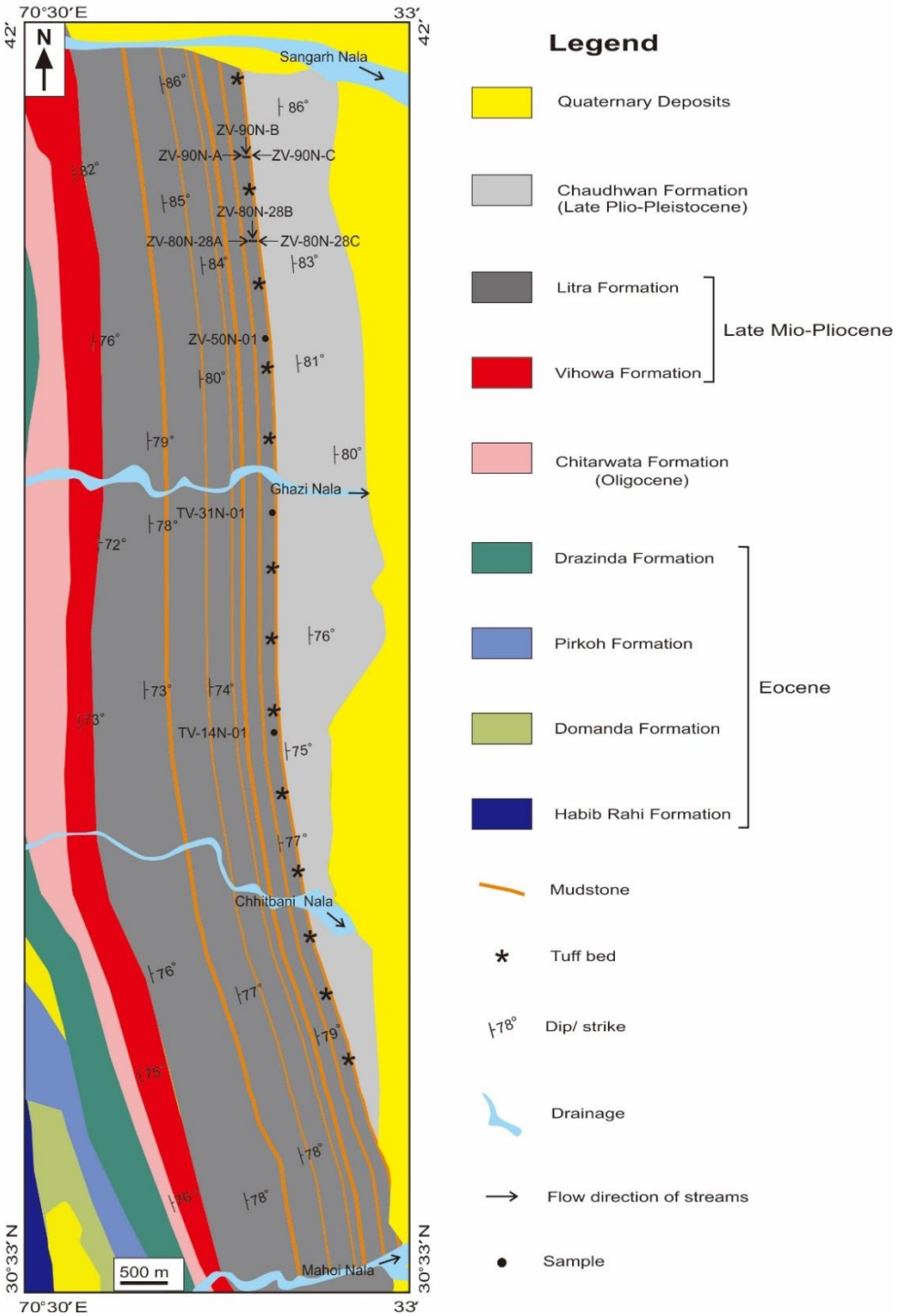

Fig. 2 Geological map of the study area (modified from Hassan, 2002) showing tuff bed and location of the investigated samples.

procedures as described in c. Suspended clay was carefully pipetted on a glass slide and air dried at ambient temperature. After scanning, the air dried sample was saturated with ethylene glycol by vapor treatment method and then was scanned again. The clay mounts were heated up to 400^0 C and 500^0 C and scanned each time.

Scanning of the oriented clay samples was carried out using PANalytical (X'Pert-3) X-ray diffractometer with Ni-filtered Cu Kα radiation (1.5404 Å), whereas scanning of the bulk samples was undertaken with PANalytical (X'Pert-PRO) X-ray diffractometer with Ni-filtered Co Kα radiation (1.7890 Å). XRD patterns were recorded over the 3° to 70° 2θ range for the bulk samples, and over 3° to 40° 2θ range for the clay-size fractions at a scan rate of 2.4° 2θ/min in continuous mode. Clay minerals were identified through their characteristic diffractions described by Moore and Reynolds (1997) and by Poppe et al. (2001), while minerals in the bulk samples were identified with the latest digital PDF (Powder Diffraction File) database of minerals. Illite crystallinity (Δ□ 2θ) based on Kubler Index (Kubler, 1968) representing full width at half maximum height of illite (001) peak at 10 Å of three untreated clay samples was determined using Origin 9 and X'Pert High Score Plus softwares.

Results and Discussion

Field Observations

The tuff bed is greyish white on fresh surface, while slightly brownish grey on the weathered surface. Its thickness ranges from less than 1 m to 3 m and it extends for about 12 km from Sangarh Nala in the north up to Chhitbani Nala in the south (Fig. 2). However, it is prominently exposed in Zamdani Nala section, two km towards south from Sangarh Nala. Here it appears as a nearly vertical cliff (Fig. 3) along the gulley eroded into the loose overlying marker mudstone. Texturally, the bed is fine-grained to silty at the bottom and clayey towards top, thus showing a fining-up grain size variation. At the bottom it shows parallel lamination, at the centre it is more or less massive but at the top it is massive, especially at Zamdani Nala section. At Ghazi Nala and farther south, it is relatively silty where the upper bedding

Fig. 3 Photographs showing tuff bed at different sites along strike; (a) top of tuff bed showing strong fracturing, which indicates brittle character of the tuff; (b) lower contact with fine-grained sandstone and upper contact with mudstone (shrubs grown on mudstone); (c) whitish fresh surface of tuff bed; (d) bore structures (bioturbation) indicating early compaction; (e) rootlets (?) with preserved organic matter; (f) colour variations in the tuff; the colour gets progressively lighter upwards (g) relatively less exposed tuff bed ~7 km southward from sites of (a) to (f); (h) close-up of (g) showing lamination in tuff bed; (i) blocky upper contact of tuff bed with mudstone.

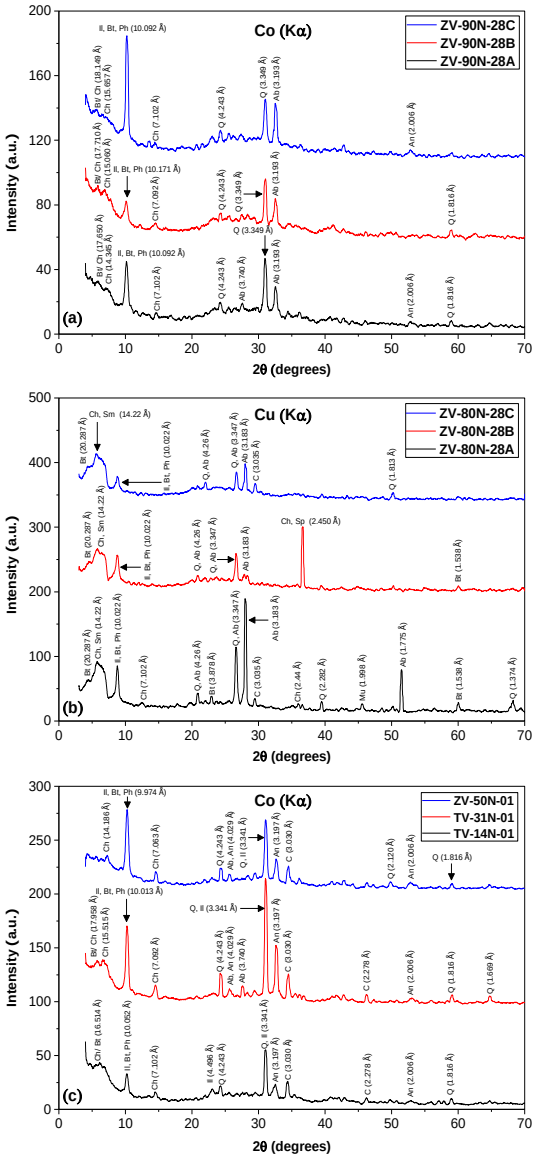

Fig. 4. XRD scans of the bulk samples of the tuff bed representing different sites along strike and bottom, centre and top of the bed at a given site. (a) bottom (ZV-90N-A), centre (ZV-90N-B), and top (ZV-90N-C), (b) bottom (ZV-80N-28A), centre (ZV-80N-28B), and top (ZV-80N-28C), (c) centre of samples (ZV-14N-01, TV-31N-01, and TV-50N-01). (Sm-smectite, Ch-chlorite, Bt-biotite, Ph-phlogopite, Il-illite, Q-Quartz, An-anorthite, Ab-albite, C-calcite, Sp-spinel).

plane is blocky and uneven probably due to the buoyant, i.e., less denser character of the tuff.

The low specific gravity of the tuff can easily be differentiated in hand samples from the associated sandstone and mudstone. It shows some bioturbation structures such as borings and rootlets (Fig. 3) The presence of bore structures suggests that the tuff bed had undergone an early compaction. Severe fracturing and jointing in the tuff bed relative to the adjacent sandstone and mudstone reflect the highly brittle behaviour of the tuff. Due to silty to clayey nature, the constituent minerals can hardly be seen megascopically except in samples from the lower part of the bed where alignment of abundant black mica probably biotite has produced parallel lamination. However, the gritty nature of the samples between the teeth implies that tuff contains silt-size quartz grains (Tucker, 2003) even in the upper clayey part. Biotite can be seen under microscope even in the upper clayey part but with very little amounts. Apparently petrography does not indicate any shards in the tuff bed, i.e., the broken glassy fragments associated with the vesicular lava, and hence the petrographic confirmation of the volcanic nature of the tuff bed is difficult.

X Ray Diffraction (XRD)

Bulk Samples Investigation

The whole-rock XRD patterns indicate that the tuffaceous bed is made up of quartz, feldspars, biotite/ phlogopite, calcite and clays (Fig. 4). The quartz appears to be low-quartz as indicated by the prominent peak at 3.34 Å. Presence of peaks at 3.18 Å and 3.19 Å indicates that feldspar is mainly plagioclase, while the lack of peak at 3.24 Å suggests absence of alkali-feldspar from the ash bed (Moore and Reynolds, 1997). Volcanic ash from Andean-type volcanism may contain abundant plagioclase feldspar due to its calc-alkaline nature. Abundant feldsapr (70 vol. %) including plagioclase with ~47 vol. % was determined in ash of Redoubt volcano of the Aleutian arc (Alaska, U.S.A.) during its eruption on December 15, 1989 (Bayhurst, et al. (1994), while the glass is the second most abundant constituent with ~29 vol. %. Other minerals in volcanic ash of Redoubt Volcano include hornblende, micas including clays, pyroxene, quartz, and magnetite.

The occurrence of biotite and/ or phlogopite is indicated by the (001) peak at 10.05 Å–10.08 Å (Fig. 4) (Kato et al., 1979; Brigatti et al., 1993). The broader peaks at 14 Å (Fig. 4) represent chlorite and smectite group clay minerals (Moore and Reynolds, 1997) Biotite and chlorite are also shown by the presence of 060 plane at 1.58 Å and 1.549 Å, respectively (Bailey, 1980). The sharp peaks at 1.77 Å (Fig. 4) may indicate spinel (Menegazzo and Carbonin, 1998).

Volcanic ash may contain silicate minerals, both coloured and colourless types, and a variety of metal oxide phases (Nakagawa and Ohba, 2002). The coloured silicates from around the world include minerals of the pyroxene, amphibole and mica groups, while the colorless minerals consist of feldspars and quartz. Besides, Fe-Ti oxide minerals such as Ti-magnetite and ilmenite are found in almost all the world occurrences of volcanic ash (Nakagawa and Ohba, 2002). The presence of biotite in the bulk sample XRD patterns supports the occurrence of abundant black mica defining lamination, especially in the lower part of the tuff bed. Biotite is an important mineral in bentonites of Kashmir basin and Potwar plateau (Johnson et al., 1984), and in Jammu area, India (Bhats et al., 2008). Biotite also occurs in significant amounts in Miocene-Quaternary volcanic

rocks (e.g., dacite) of Chagai magmatic arc (Siddiqui et al., 2015). Abundance of the quartz in XRD patterns confirms the gritty character of the hand samples which is a field-based test for the presence of silty or sandy quartz in mudstones (Folk, 2003). Calcite seems to increase in the tuff bed from north to south (Fig. 4) as indicated by the absence of its characteristic peak at 3.03 Å in samples ZV-90A to ZV-90C, the northernmost samples (Fig. 2), and by a relatively good peak at 3.03 Å in samples TV-14N-01, TV-31N-01, and ZV-50N-01, which are the southerly located samples in the study area (Fig. 2). In Zamdani Nala section, which is the type section of the Taunsa tuff bed, calcite seems to be absent from the centre of the bed as there is no characteristic peak of calcite (3.03 Å) Effenberger et al., 1981) in ZV-80N-B (centre), while the lower and upper parts contain calcite as shown by XRD patterns of samples ZV-80N-A and ZV-80N-C (Fig. 4), which represent the bottom and top of the tuff bed, respectively. Calcite may be present in the tuff as a cement like in the surrounding sandstone units with abundant calcite cement. To form carbonate cement in the tuff, carbonate solutions may have been derived from the dissolution of carbonate rock fragments and carbonate bioclasts in the associated sandstone and mudstone facies or alternatively from the alteration of feldspar (plagioclase) (Pichler and Schmitt-Riegraf, 1997; Ulmer-Scholle et al., 2014) which may be present in the tuff as indicated in the XRD patterns of some of the samples (Fig. 4)

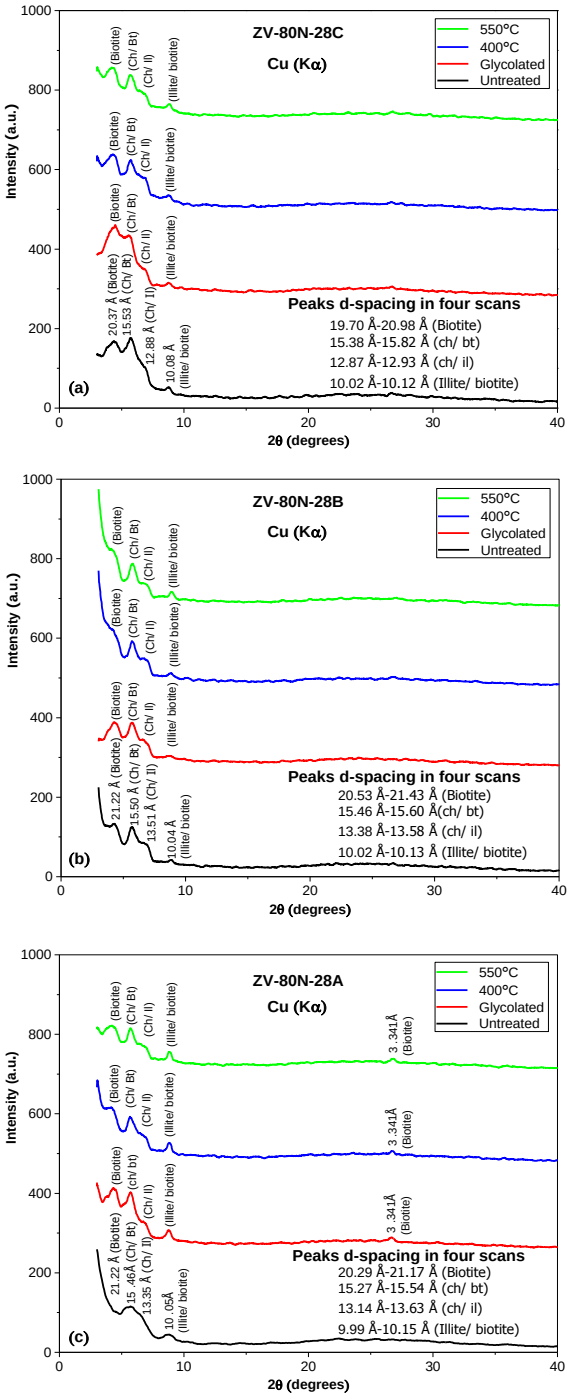

Fig. 5. XRD scans of clay-fraction samples of tuff bed representing its different parts: (a) top (ZV-80N-28C), (b) centre (ZV-80N-28B), and (c) bottom (ZV-80N-28A). (Bt-biotite, Il-illite, Ch-chlorite, Ch/Il- chlorite-illite mixed clay; Ch/Bt- chlorite/ biotite interlayered phase).

Clay Fraction Investigation

The clay scans of the Taunsa volcanic ash bed show illite, chlorite and mica (probably biotite) (Fig. 5). Biotite and muscovite occur as clay-size fraction of soil (Fordham, 1990; Moore and Reynolds, 1997; Verma et al., 2014). Biotite is found in clay fractions of the pyroclastic deposits of Mount St. Helen (Pevear et al., 1982). Presence of biotite in the Taunsa tuff bed is also confirmed by the petrographic study, especially in lower part of the bed. The 10 Å peak with 100% intensity and the very low intensity peak at ~3.35 Å peak (ZV-80N-28A) show that mica most probably is biotite rather than muscovite since the XRD pattern of the latter shows a relatively more prominent peak at 3.33 Å (Hendricks and Jefferson, 1939; Kanwano and Tomita, 1988).

Unlike bentonites, the Taunsa tuff clay scans do not show the occurrence of any discrete or mixed smectite clay. The clay scans are characterized by four peaks, i.e., ~20 Å to ~21 Å, ~15 Å to ~16 Å, ~13 Å to ~14 Å and ~10 Å (Fig. 5). The peak at ~20 Å may reflect either (R1) ordered (1:1) interlayering of illite and biotite as the XRD patterns of both these minerals are characterized by (001) peak at 10 Å that on addition can produce a superstructure with (001) at ~20 Å (Moore and Reynolds 1997). An alternate possibility could be the 100% intensity peak of 3M biotite at this position (20 Å) (Takeda and Ross, 1975). The peak ~15 Å to ~16 Å may represent random interlayering of 3M biotite with (001) peak at 20 Å and chlorite with a basal 14 Å (001) peak. The random interlayering of clay minerals is represented by peaks at positions intermediate to the nearby basal peaks. The position and symmetry of the resulting combined peaks depend on the abundance of original discrete phases (Moore and Reynolds, 1997).

The peak at ~13 Å to ~14 Å results from random interlayering of chlorite with (001) peak at 14 Å and biotite with (001) peak at 10 Å. Alternatively, the peak at ~13 Å to ~14 Å may reflect random interlayering of chlorite and illite with (001) peaks at 14 Å and 10 Å, respectively. The peak at 10 Å may represent biotite, muscovite and/ or illite since the structures of all the three possess a (001) peak at this position. Thus, biotite, chlorite, illite and mixed layer phases such as biotite/ illite, biotite/ chlorite and chlorite/ illite may be present in clay fraction of the volcanic ash bed. Small amounts of chlorite are reported in many types of pyroclastic deposits of Mount St. Helen volcano, U.S.A. (Pevear et al., 1982). Chlorite occurs interlayered with biotite (Lijima and Zhu, 1983; Olives et al., 1983) and with illite/ muscovite (Page and Wenk, 1979; Knipe, 1981; Lee et al., 1984). Mixed-layer biotite-chlorite has been widely reported and commonly attributed to the alteration of biotite (Eggleton and Banfield, 1985). Similarly, transformation of smectite to both illite and chlorite has been documented in several ash beds (Hower et al., 1976). lllite may form by (i) weathering of silicates (primarily feldspar), (ii) alteration of other clay minerals (Lynch et al., 1997), and (iii) degradation (Deer et al., 1992) or weathering of muscovite in soils (Fanning et al., 1989). Illite is reported to form from weathering of biotite in soils in United States (Nettleton et al., 1973), and in sandstone from Antarctica (Verma et al., 2014). Smectite may convert to illite at deep burial (Boles and Franks, 1979; McKinley et al., 2003). Formation of smectite resulting from the breakdown of volcanic ash (Altaner and Grim, 1990; Jeans et al., 2000) is favored by mildly alkaline conditions (e.g., marine environments) having high Si and Mg potentials (Borchardt, 1977) and availability of Ca and the paucity of K (Deer et al., 1992).

The absence of smectite in the Taunsa tuffaceous rock reflects that smectite was replaced by illite either completely or preserved in amounts too little to be indicated in XRD patterns (Fig. 5). Illite and illite-smectite composite phase are also common products of weathering and alteration, which are frequently interpreted to be the result of illitisation of the previously formed smectite (Christidis and Huff, 2009; Middleton et al., 2015). Illitisation of smectite may also produce mixed illite-smectite phase with only trace proportions of smectite.

Illite crystallinity of the Taunsa tuff bed ranges from 0.41 Å to 0.90 Å and these values correspond to deep diagenetic zone (Verdel et al., 2011), which therefore supports reworking of the tuff from a deeper unit in the stratigraphic succession of the Sulaiman Range to its present site of occurrence corresponding to shallow diagenetic zone.

In an accompanying study (unpublished) of this investigation, clay minerals characterisation of sandstone and mudstone units of the Litra Formation, and of a sandstone unit from the lower part of the Chaudhwan Formation adjacent to the tuff bed (Fig. 2) was undertaken with XRD (results of this study have not been incorporated in this article). This investigation characterises abundant smectite in the clay fraction of the sandstone samples representing both the Litra and Chaudhwan formations. The presence of smectite in sandstone represents shallow levels of burial, while its absence in the tuff bed may reflect replacement of smectite by illite during deep burial (Boles et al., 1979; McKinley et al., 1999). Thus, the presence of illite in the Taunsa tuff bed suggests its derivation from an earlier volcanic ash occurrence in the deeper diagenetic zone where smectite phase may have been replaced by illite.

The reworked nature of the Taunsa tuff is also obvious from the presence of sedimentary lamination, especially in the lower part of the tuff bed as discussed before.

Source of Volcanic Ash

As the Himalayas have no reported syn- and late-orogenic volcanism, there should be an outside source of volcanism to contribute volcanic ash to Siwaliks (Johnson et al., 1982). It seems that volcanic eruptions of Dacht-e-Nawar complex in Afghanistan may have contributed ashfall deposits to Upper Siwaliks in Potwar plateau and Kashmir basin (Johnson et al., 1982; Bhat et al., 2008). This is also indicated by similar fission track ages of 2.86 m.y. to 1.608 m.y. of the volcanic tuff in Upper Siwaliks (Johnson et al., 1982), and by the K-Ar ages of 2.88 m.y. to 1.68 m.y. of Dacht-e-Nawar complex (Bordet, 1975). However, the oldest bentonites occurring in the Nagri Formation of the Siwalik Group in Potwar plateau have a fission track age of 9.46 m.y. (Johnson et al., 1982), which is also older than the reported eruptive history of Dacht-e-Nawar volcanoes that ranges from Miocene (i.e., ~5 m.y.) to Quaternary (Johnson et al., 1982, references therein). This older bentonite may indicate an earlier but unreported phase of volcanic eruption in Dacht-e-Nawar volcanic complex or alternatively some other source of volcanic ash possibly one related to Chagai arc which has a more prolonged volcanic history from Cretaceous to Quaternary (Khan et al., 2010; Nicholson et al., 2010). The late Cretaceous-Paleocene volcanic suite of Chagai arc has formed in intra-oceanic arc setting, while the Oligocene-Quaternary volcanics formed in continental setting (Siddiqui et al., 2009). The mineralogy and geochemistry of the Plio-Pleistocene volcanic rocks of Chagai arc (Siddiqui et al., 2009) are similar to Taunsa tuff, but the former seems unlikely to have supplied ash to the latter because of its reworked nature. The older ashfall deposits to be reworked may belong to an Eocene-Oligocene age volcanism (Siddiqui et al., 2015).

The volcanic ash deposits occurring in the late Cretaceous Bibai volcanic rocks to have been subsequently reworked to form the Taunsa tuff also

seem unlikely on the basis of geochemical differences between Bibai volcanics which are basaltic in composition (Siddiqui et al., 2010) and the Taunsa tuff which is andesitic to dacitic in composition (unpublished).

An earlier pre-Quaternary phase of volcanic eruption is evidenced by the tuff occurrences in Eocene age rocks from northwestern Himalayas in India (Mehra et al., 1990; Pandey et al., 2014). The source of these ashfall deposits is considered to belong to Dacht-e-Nawar volcanic complex of Afghanistan (Pandey et al., 2014, references therein). A tuffaceous siltstone occurring in Eocene age Dharamsala Formation from Tileli area, Mandi District, Himachal Pradesh, India (Pandey et al., 2014) has an andesitic-dacitic composition like Taunsa tuff, and the Tileli tuff is composed of biotite, muscovite (illite), chlorite and hematite phases (Pandey et al., 2014). Thus, this tuffaceous deposit seems to correlate with Taunsa ash bed both mineralogically and compositionally. Based on analogous occurrences of volcanic ash both in Pakistani and Indian Siwaliks (Johnson et al. 1982; Bhat et al., 2008), it can be inferred that an equivalent volcanic ash may also occur in Eocene rocks in Pakistani Himalayas, and possibly also in Sulaiman Range. Such as an older volcanic ash occurring within the pre-Siwalik units of the Sulaiman Range might have led to the origin of the Taunsa tuff upon reworking.

Chagai magmatic arc seems to be a more likely source of the Taunsa tuff and other possible occurrences elsewhere in Sulaiman and Kirther ranges, as suggested, due to several reasons: (i) the presence of andesitic to rhyodacitic rocks in Chagai magmatic arc (ii) prolonged volcanic history of the Chagai arc from Cretaceous to Quaternary (Khan et al., 2010; Nicholson et al., 2010) and (iii) much closer proximity of the Chagai arc to Sulaiman and Kirther ranges than to Kashmir and Potwar areas (Fig. 1). However, radiometric dating and SEM investigation of the Taunsa tuff may confirm the preliminary findings of this research. Furthermore, volcaniclastic deposits occurring in Balochistan Basin, especially the post-Eocene occurrences, may be searched in Sulaiman Range which may provide more constraints on the origin of the Taunsa tuff.

Conclusion

The presence of parallel lamination indicates the reworked nature of the Taunsa tuff. Like the tuffaceous bentonites of Potwar plateau and Kashmir basin, the Taunsa tuff contains abundant biotite. However, absence of smectite in the latter makes it different from the former two examples. Taunsa tuff bed is characterized by quartz, feldspars, calcite and phyllosilicate phases such as illite, chlorite, biotite and mixed-layer clays. The presence of abundant smectite in the clay-size fractions of the associated sandstone units of the tuff indicates the shallow zone of diagenesis, while the illite crystallinity suggests the deep burial of the tuff, which implies the reworked nature of the Taunsa tuff. As the Indian occurrences exemplify, a precursor ashfall deposit may occur in a pre-Siwalik unit of the Sulaiman Range which might have led to the sedimentation of the Taunsa tuff upon reworking. The source of the volcanic ash may belong more likely to Chagai arc in Pakistan or less likely to Dacht-e-Nawar volcanic complex in Afghanistan.

Acknowledgement

The authors thank the management of Pakistan Atomic Energy Commission for funding the research, and for their moral support. Special thanks are due to Prof. Muhammad Arif, Department of Geology, University of Peshawar, and an anonymous foreign reviewer who suggested many valuable changes both in the content and language of the manuscript. Help of the technicians in the field and laboratory works is also acknowledged.

References

Ahmad, W., Khan, M. J. (1991). Petrography of the upper Litra and Chaudhwan formations, upper Siwalik Group, Zindapir anticline, Northern Sulaiman Range. *Journal of Himalayan Earth Sciences*, **24**, 191–202

Altaner, S. P., Grim, R. E. (1990). Mineralogy, chemistry, and diagenesis of tuffs in the Sucker Creek Formation (Miocene), eastern Oregon. *Clays and clay Minerals*, **38**(6), 561–572.

Arif, M., Mazhar, F., Mujeeb-ur-Rahman, Ullah, R. (2005). Mineralogy and chemistry of volcanic clay (fuller's earth) from Taunsa area, Dera Ghazi Khan, Pakistan. [Abstract]. *Journal of Himalayan Earth Sciences*

Asim, S., Qureshi, S. N., Mirza, Q., Saleem, U. Ali, S., Haroon, M., Tahir, M. (2014). Structural and stratigraphic interpretation of seismic profiles along Safed Koh Trend, Eastern Part of Sulaiman Fold Belt, Pakistan. *Universal Journal of Engineering Science*, **2**(4), 77–95.

Aziz, M. Z, Khan M. R. (2003). A review of Infra-Cambrian source rock potential in Eastern Sindh, an analogue to Huqf Group of Oman. *Infra-Cambrian play of Eastern Sindh, Pakistan.*

Bailey, S. W. (1980). Structures of layer silicates; in Brindley, G. W., and Brown, G. editors, Crystal Structures of Clay Minerals and their X-ray Identification. Monograph 5. *Mineralogical Society, London*, 1–123.

Banks, C. J., Warburton, J. (1986). Passive roof duplex geometry in the frontal structures of the Kirthar and Sulaiman Mountain belts, Pakistan. *Journal of Structural Geology,* **8,** 229–237.

Bayhurst, G. K., Wohletz, K. H., Mason, A. S. (1994). A method for characterising volcanic ash from the December 15, 1989 eruption of Redoubt volcano, Alaska. *U.S. Geological Survey Bulletin* 2047

Bhat, G. M., Kundal, S. N., Pandita, S. K., Prasad, G. V. R. (2008). Depositional origin of tuffaceous units in the Pliocene upper Siwalik Subgroup, Jammu (India), NW Himalaya. *Geological Magazine*, **145**(2), 279–294.

Bhola, K. L. (1948). Bentonite in India. *Quarterly Journal of Geological, Mining, and Metallurgical Society, India*, **19,** 55–77.

Boles, J. R., Franks, S. G. (1979). Clay diagenesis in Wilcox sandstones of Southwest Texas; implications of smectite diagenesis on sandstone cementation. *Journal of Sedimentary Research*, **49**(1), 55–70.

Borchardt, G. A. (1977). Montmorillonite and other smectite minerals. *Minerals in Soil Environments*, 293–330.

Bordet, P. (1975). Les volcans recents du Dacht-e-Nawar (Afghanistan central). Ann. Sci. Univ. Clermont. *Geology and Mineralogy*, **26**, 1–86

Brigatti, M. F., Poppi, L. (1993). Crystal chemistry of Ba-rich trioctahedral micas-1M. *European Journal of Mineralogy, 5, 856*

Christidis, G. E., Huff, W. D. (2009). Geological aspects and genesis of bentonites. *Elements,* **5**, 93–98.

Deer, W. A., Howie, R. A., Zussman, J. (1992). *An introduction to the rock-forming minerals*: Essex. England: Longman Scientific and Technology.

Effenberger, H., Mereiter, K., Zemann, J. (1981). Crystal structure refinements of magnesite, calcite, rhodochrosite, siderite, smithonite, and dolomite, with discussion of some aspects of the stereochemistry of calcite type carbonates. *Zeitschrift für Kristallographie-Crystalline Materials*, **156**(1–4), 233–244.

Eggleton R. A., Banfield J. F. (1985). The alteration of granitic biotite to chlorite. *American Mineralogist*, **70**, 902–910.

Fanning, D. S., Keramidas, V. Z., El-Desoky, M. A. (1989). Micas. *Minerals in Soil Environments*, **1**, 551–634.

Fordham, A. W. (1990). Formation of trioctahedral illite from biotite in a soil profile over granite gneiss. *Clays and Clay Minerals*, **38**(2), 187–195.

Haq, S. S. B., Davis, D. M. (1997). Oblique convergence and the lobate mountain belts of western Pakistan. *Geology*, **25**, 23–26.

Hassan, M. U. (2002). Geological map of Dera Ghazi Khan quadrangle (39J), Punjab, Pakistan. Quetta: Geological Survey of Pakistan

Hendricks, S. B., Jefferson, M. E. (1939). Polymorphism of the micas with optical measurements. *American Mineralogist*, **24**(12), 729–771.

Hower, J., Eslinger, E., Hower, M. E., Perry, E. A. (1976). Mechanism of burial metamorphism of argillaceous sediments: Mineralogical and chemical evidence. *Geological Society of America Bulletin*, **87**, 725–737.

Humayon, M., Lillie, R. J., Lawrence, R. D. (1991). Structural interpretation of the eastern Sulaiman fold belt and foredeep, Pakistan. *Tectonics*, **10**, 299–324.

Iqbal, M., Helmcke, D. (2004). Geological interpretation of earthquakes data of Zindapir anticlinorium, Sulaiman Fold belt, Pakistan. *Pakistan journal of Hydrocarbons Research*, **14**, 41–47

Jackson, M. L. (1978). Soil chemical analyses. Authors' publication, University of Wisconsin, Madison

Jadoon, I. A. K., Lawrence, R. D. Lillie, R. J. (1994). Seismic data, geometry, evolution and shortening in the active Sulaiman fold-and-thrust belt of Pakistan. *American Association of Petroleum Geologists Bulletin*, **78**, 758–774.

Jeans, C. V., Wray, D. S., Merriman, R. J., Fisher, M. J. (2000). Volcanogenic clays in Jurassic and Cretaceous strata of England and the North Sea Basin. *Clay Minerals*, **35**(1), 25–55.

Johnson, G. D., Zeitler, P., Naeser, C. W., Johnson, N. M., Summers, D. M., Frost, C. D., ... Tahirkheli, R. A. K. (1982). The occurrence and fission-track ages of Late Neogene and Quaternary volcanic sediments, Siwalik Group, northern Pakistan. *Palaeogeography, Palaeoclimatology, Palaeoecology*, **37**(1), 63–93.

Kanwano, M., Tomita, K. (1988). Ammonium-bearing dioctahedral 2M1 mica from Aira district, Kagoshima Prefecture. *Clay Science*, **7**(3), 161-169.

Kato, T., Miura, Y., Yoshii, M., Maeda, K. (1979). The crystal structures of 1M-kinoshitalite, a new barium brittle mica and 1M-manganese trioctahedral micas. *Mineralogical Journal*, **9**(7), 392–408.

Kazmi, A. H. (1988). Stratigraphy of The Dungan Group in Kach-Ziarat area, NE Balochistan. *Journal of Himalayan Earth Sciences*, **21**, 117–130.

Kemal, A., Balkwill, H. R., Stoakes, F. A. (1991). Indus basin hydrocarbon play: New directions and strategies for accelerating petroleum exploration and production in Pakistan. *Proceedings of International Petroleum Seminar* (pp. 78–105). Islamabad

Khan, M. A., Siddiqui, R. H., Jan, M. Q. (2010). Temporal evolution of Cretaceous to Pleistocene magmatism in the Chagai Arc, Balochistan, Pakistan. *Proceedings for the 25th Himalaya-Karakoram-Tibet Workshop*: U.S. (p. 2).

Knipe R. J. (1981). The interaction of deformation and metamorphism in slates. *Tectonophysics* **78,** 249–292

Kubler, B. (1968). Evaluation quantitative du métamorphisme par la cristallinité de I'illite. *Bulletin Centre de Researches de Pau*-SNPA, ***2***, 385–397.

Lee, J. H., Peacor, D. R., Lewis, D. D., Wintsch, R. P. (1984). Chlorite-illite/muscovite interlayered and interstratified crystals: a TEM/STEM study. *Contributions to Mineralogy and Petrology*, **88**(4), 372–385.

Lijima, S., Zhu, J. (1982). Electron microscopy of a muscovite–biotite interface. *American Mineralogist*, **67**(11–12), 1195–1205.

Lynch, F. L., Mack, L. E., Land, L. S. (1997). Burial diagenesis of illite/smectite in shales and the origins of authigenic quartz and secondary porosity in sandstones. *Geochimica et Cosmochimica Acta*, **61**(10), 1995–2006.

McKinley, J. M., Worden, R. H., Ruffell, A. H. (1999). Smectite in sandstones: a review of the controls on occurrence and behaviour during diagenesis. In R. H. Worden & S. Morad (Eds.), *Clay mineral cements in sandstones*, (pp. 109–128). Oxford: Wiley-Blackwell

Mehra, S., Misra, V. P., Mathur, A. K. (1990). Biostratigraphic studies of Lower Tertiary sequence particularly in the Dagshai-Kasauli Formations of HP. *Geological Survey India*, **123**, 258–260.

Menegazzo, G., Carbonin, S. (1998). Oxidation mechanisms in Al-Mg-Fe spinels: A second stage α-Fe_2O_3 exsolution. *Physics and Chemistry of Minerals*, **25**(8), 541–547.

Middlemiss, C. S. (1930). *Jammu and Kashmir Minerals Survey Report,* pp. 32–37.

Middleton, A. W., Uysal, I. T., Golding, S. D. (2015). Chemical and mineralogical characterization of illite-smectite: implications for episodic tectonism and associated fluid flow, central Australia. *Geochimica et Cosmochimica Acta,* **148**, 284–303.

Moore, D. M., Reynolds Jr, R. C. (1997). *X-ray diffraction and the identification and analysis of clay minerals*. Oxford: Oxford University Press.

Najman, Y. (2006). The detrital record of orogenesis: A review of approaches and techniques used in the Himalayan sedimentary basins. *Earth Science Reviews,***74**(1–2), 1–72.

Nakagawa, M. I., Ohba, T. (2002). Minerals in volcanic ash 1: Primary minerals and volcanic glass. *Global Environmental Research (*English Edition), **6**(2), 41–52.

Nettleton, W. D., Nelson, R. E., Flach, K. W. (1973). Formation of mica in surface horizons of dryland soils: *Proceedings of Soil Science Society of America*, **37**, 473–478.

Nicholson, K. N., Khan, M., Mahmood, K. (2010). Geochemistry of the Chagai–Raskoh arc, Pakistan: Complex arc dynamics spanning the Cretaceous to the Quaternary. *Lithos*, **118**(3–4), 338–348.

Olives B. J., Amouric M., de Fouquet C., Baronnet A. (1983). Interlayering and interlayer slip in biotite as seem by HRTM. *American Mineralogist*, **68**, 754– 758.

Page, R., Wenk, H. R. (1979). Phyllosilicate alteration of plagioclase studied by transmission electron microscopy. *Geology*, **7**, 393–397.

Pandey, P., Chabbra, J., Joshi, G. B., Parihar, P. S. (2014). Occurrence of tephra/volcanic tuff in the tertiary sediments of Himachal Himalaya from Tileli area, Mandi district, HP: Implication for stratigraphy and uranium mineralization. *Journal of the Geological Society of India*, **83**(1), 5–12.

Pevear, D. R., Dethier, D. P., Frank, D. (1982). Clay minerals in the 1980 deposits from Mount St. Helens. *Clays and Clay Minerals*, **30**(4), 241–252.

Pichler, H., Schmitt-Riegraf, C. (1997). *Rock-forming minerals in thin section*. London, New York, Madras: Chapman & Hall.

Poppe, L. J., Paskevich, V. F., Hathaway, J. C., Blackwood, D. S. (2001). *A laboratory manual for X-ray powder diffraction.* (**1**-041). U.S. Geological Survey

Saif-Ur-Rehman, K. J., Ding, L., Jadoon, I. A., Idrees, M., Zaib, M. O. (2020). Geometry and development of Zindapir Anticlinorium, Sulaiman

Range, Pakistan. *Journal of Structural Geology*, **131**, 103932.

Siddiqui, R. H., Brohi, I. A., Haidar, N. (2010). Geochemistry, petrogenesis and crustal contamination of Hotspot related volcanism on the northwestern margin of the Indian continent and its implications for paleosedimentary environments. *Sindh University Research Journal-SURJ (Science series)*, **42**(2).

Siddiqui, R. H., Khan, M. A., Jan, M. Q., Kakar, M. I., Kerr, A. C. (2015). Geochemistry and petrogenesis of Oligocene volcaniclastic rocks from the Chagai arc: implications for the emplacement of porphyry copper deposits. *Arabian Journal of Geosciences,* **8**(10), 8655–8667.

Siddiqui, R. H., Khan, M. A., Jan, M. Q., Ogasawara, M. (2009). Petrogenesis of Plio-Pleistocene volcanic rocks from the Chagai arc, Balochistan, Pakistan. *Journal of Himalayan Earth Sciences*, 1–24.

Takeda, H., Ross, M. (1975). Mica polytypism: dissimilarities in the crystal structures of coexisting 1M and 2 M1 biotite. *American Mineralogist*, **60**(11–12), 1030–1040.

Tucker, M. E. (2003). Sedimentary rocks in the field. Chichester, West Sussex, UK: John Wiley & Sons.

Ulmer-Scholle, D. S., Scholle, P. A., Schieber, J., Raine, R. J. (2014). A color guide to the petrography of sandstones, siltstones, shales and associated rocks. *American Association of Petroleum Geologists*, Memoir 109.

Verdel, C., Niemi, N., Van Der Pluijm, B. A. (2011). Variations in the illite to muscovite transition related to metamorphic conditions and detrital muscovite content: insight from the Paleozoic passive margin of the southwestern United States. *The Journal of Geology*, **119**(4), 419–437.

Verma, K., Bhattacharya, S., Ansari, A. A., Srivastava, P. K., Dharwadkar, A. (2014). Geomorphic control on the formation of mixed layer clays by progressive degradation of biotite: A case study from Jutulsessen Gjelsvikfjella, East Antarctica. *Journal of the Geological Society of India,* **83**(5), 532–534.